Model Predictive Control leveraging Ensemble Kalman Forecasting for optimal power take-off in wave energy conversion systems

Daniele Cavaglieri, Thomas R. Bewley, and Mirko Previsic

Abstract—Although solar and wind energy are the dominant sources of renewable energy production today, attention is increasing towards other solutions, such as marine Wave Energy Conversion (WEC). High installation costs and the relatively low efficiency of current power take-off mechanisms currently prevent WEC from being competitive with solar and wind energy production. One potential way to overcome this is by implementing an active control strategy which optimizes WEC power takeoff in real time, thereby extracting the maximum energy possible from each individual wave. Accomplishing this requires an estimation problem to be solved, since oncoming sea waves are not known a priori—they come from multiple directions, and generally arrive in sets. In the present work, a parallel Ensemble Kalman forecasting algorithm leveraging a pseudospectral wave model for time propagation of the ensemble members is developed to estimate and forecast the wavefield based on data assimilated from a Doppler wave radar system. This forecast of the future wavefield is then exploited in a linear Model Predictive Control (MPC) setting for the online optimization of power take-off of a one-body point-absorber WEC system subject to motion and machinery constraints. Simulations over a realistic sea state exhibit a trade-off between control efficiency and forecast accuracy, with power losses in the prediction-based setting not exceeding 16% of the power take-off obtained using MPC under the ideal assumption of complete knowledge of the oncoming wavefield.

I. INTRODUCTION

Most discussions of renewable energy production focus on solar and wind. Only recently has increased attention turned towards wave energy conversion (WEC) in the ocean. WEC is zero-emission and essentially non-intermittent, as opposed to solar and wind energy sources, and can be implemented with minimal visual and environmental impact. However, the installation and maintenance costs of modern WEC devices, together with their relatively low energy production, currently prevent WEC from being competitive with more mature fields of renewable energy production. One way to overcome this is to improve the power take-off strategy in such devices, which currently relies on a suboptimal tuning approach designed to match the resonance frequency of the device to the peak of the average wave spectrum at the operating location, and limits the motion of the device based on a highly-conservative estimate of worst-case wave heights at the current sea state. By implementing an active controller which adapts the power take-off parameters to the oncoming wavefield, the performance of WEC devices can be significantly improved.

This work has been supported by an NSF grant to ReVision Consulting. D. Cavaglieri and T.R. Bewley are with the Flow Control Lab, Dept of MAE, UC San Diego, La Jolla, CA 92093-0411 {dcavagli@ucsd.edu, bewley@ucsd.edu}. M. Previsic is with ReVision Consulting, 1104 Corporate Way, Sacramento, CA, 95831 {mirko@re-vision.net}

Over the years, many active control schemes have appeared in literature, though the majority of them do not realistically facilitate implementation, due to the simplifying assumptions upon which their theoretical derivation is based, eventually leading to suboptimal solutions to the power takeoff tuning problem. One of the earliest results, denoted complex-conjugate control (see [1] for a review), considers the optimization of the energy absorption of a point-absorber WEC device oscillating in heave only, which is obtained by matching the machinery impedance $Z_m(\omega)$ with the complex conjugate of the device's intrinsic impedance $Z_i^*(\omega)$. The control law so derived is inherently noncausal, and practical implementation appears infeasible. Several attempts have been made to modify this formulation to produce a causal realization of such a control approach. One of the most promising such approaches, denoted optimal velocity tracking, calculates the optimal velocity v^{opt} to impose to the device with respect to the wave excitation force $F_e(\omega)$ acting on the device due to its interaction with the wavefield. Denoting with $R_i(\omega)$ the radiation resistance of the device, the optimal device velocity is determined as $v^{opt} = F_e(\omega)/(2R_i(\omega))$. Due to the noncausality of the excitation force, a concept that will be explained in greater detail in Section II, this control approach does not lead to a practical implementation, unless knowledge of the future excitation force is available. Moreover, all of the approaches just mentioned, which are also referred to as reactive control, do not handle well the case in which the WEC device is composed by multiple bodies, or it is subject to machinery and motion constraints.

Other control approaches which instead do not require reactive power, are latching and clutching control. The basic idea underlying latching control is to lock the device motion when the device velocity becomes zeros during the wave oscillating cycle (latching) and let the device free to oscillate in phase with the excitation force in other parts of the wave cycle (unlatching). Clutching control, instead, works by repeatedly coupling and decoupling (clutching) the machinery load during the oscillating cycle according to a defined control rule. Such control techniques present however obvious structural implementation problems. Besides, the determination of the unlatching or clutching instants is strongly affected by the regularity of the oncoming waves and has been observed to change according to the wave height and wave period, further precluding a straightforward implementation.

Model Predictive Control (MPC), on the other side, represents an extremely flexible approach, in which the

optimal control maximizing the WEC power take-off over a predefined control optimization horizon T_h is calculated through the online solution of an optimization problem. In this framework, any WEC device subject to linear dynamics and linear constraints can be handled in the same way, and the determination of the optimal control law requires at each instant the solution of a quadratic programming problem. Moreover, in [2] a comparison of the control schemes here briefly described has been performed, and simulations considering a one-body point absorber WEC device under representative sea conditions have proved that MPC is the solution providing, on average, maximum power take-off. However, a practical implementation of such approach requires knowledge of the future excitation force for the correct representation of the system dynamics over the control horizon, hence a forecasting problem arises. Interestingly, few attempts have appeared so far in literature at providing a reliable estimate of wave interaction force to be leveraged in the MPC setting. Amongst them, Hals et al [3] developed an augmented Kalman filter with a damped harmonic oscillator as model for the propagation of a onedimensional wavefield.

The present work aims at deriving a feasible MPC approach leveraging actual wave measurements for the prediction of the excitation force over the control horizon. The organization of the paper is as follows: Section II describes the dynamic model of a one-body point-absorber WEC in heave. Such model will be used to assess the performance of our prediction-based MPC approach. Section III introduces Ensemble Kalman Forecasting (EnKF) for the estimation of the future wavefield leveraging wave data measurement. In Section IV, wave prediction is leveraged in a Model Predictive Control framework in order to calculate the optimal control law maximizing the power take-off of a WEC device. Finally, in Section V, we analyze the effect that EnKF wave forecasting, coupled with MPC, has on the power take-off of a one-body point-absorber, and we compare the results with the case in which the future wavefield is known a priori.

II. WAVE ENERGY CONVERTER MODEL

Many WEC topologies have appeared in literature, a few of them allowing the possibility of an active controller. Among these, the linear one-body point-absorber subject to heave motion only, due to the simplicity of the power extraction mechanism, has received the greatest attention in literature. This converter is composed by a semisubmerged floating body, which is fixed to the sea bottom through a connection containing a linear drive actuator. Such device, in the hypothesis of negligible nonlinear effects, is subject to an inertial force, a viscous force, due to hydrodynamic friction, a buoyancy force, proportional to the device displacement according to Archimedes' principle, a radiation force $f_R(t)$ capturing the effect that the device motion has on a volume of still water in which it is immersed, and an excitation force $f_e(t)$ which represents the effect that the wavefield has on the device, considered still. Besides, a control force u(t) is considered to be applied to the device. Denoting with z(t)

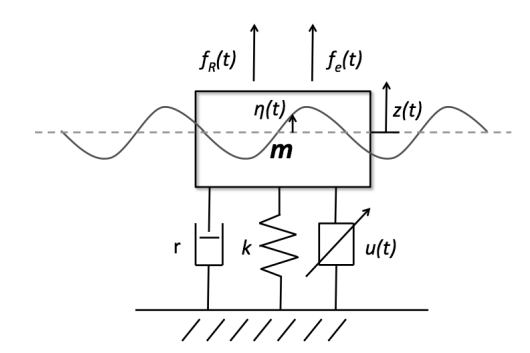


Fig. 1: Model of a one-body point absorber WEC device

the WEC heaving displacement, the balance of forces on the device, as shown in Figure 1, gives:

$$m \ddot{z}(t) + r \dot{z}(t) + k z(t) = f_R(t) + u(t) + f_e(t)$$
 (1)

where m is the device mass, r is the viscous damping, and k is the buoyancy stiffness, defined as $k=\rho gS$, where ρ is the water density, g the gravitational constant, and S the water plane area. The radiation force $f_R(t)$, according to [4], can be expressed as

$$f_R(t) = -m_\infty \ddot{z}(t) - f_r(t)$$

$$= -m_\infty \ddot{z}(t) - \int_{-\infty}^t h_r(t - \tau) \dot{z}(\tau) d\tau$$
(2)

where m_{∞} is the added mass, $f_r(t)$ is the reduced radiation force, and $h_r(t)$ is the impulse response function of the reduced radiation force. For simplicity, in the rest of the paper we will refer to the term $f_r(t)$ as the radiation force. The excitation force $f_e(t)$ is expressed as

$$f_e(t) = \int_{-\infty}^{+\infty} h_e(t - \tau) \,\bar{\eta}(\tau) \,d\tau \tag{3}$$

where $h_e(t)$ is the excitation force impulse response function, and $\bar{\eta}(t)$ is the wave elevation time series at the device location. As mentioned in [4], the impulse response function relating the wave elevation to the excitation force affecting the device happens to be noncausal. The main reason is that the chosen input, i.e. the wave elevation at the device location, is not the direct cause of the output, i.e. the interaction force between the wavefield and the device. The actual cause of the output may be a storm far away, and the interposed wavefield is only a means through which such input propagates, hence the loss of causality.

In order to recast the system dynamics into state-space form, the radiation force $f_r(t)$ in (2) can be discretized through the following state-space realization [4]:

$$\begin{cases} \dot{X}_r(t) = A_r \, X_r(t) + B_r \, \dot{z}(t) \\ f_r(t) = C_r \, X_r(t) + D_r \, \dot{z}(t) \end{cases} \tag{4}$$

This leads to the following state-space model:

$$\dot{x}(t) = A x(t) + B u(t) + B f_e(t)$$
 (5)

with

$$A = \begin{bmatrix} A_r & 0 & B_r \\ 0 & 0 & I \\ -\frac{C_r}{m+m_{\infty}} & -\frac{k}{m+m_{\infty}} & -\frac{r+D_r}{m+m_{\infty}} \end{bmatrix}, B = \begin{bmatrix} 0 \\ 0 \\ \frac{1}{m+m_{\infty}} \end{bmatrix}$$
(6)

where x is the state-space vector containing the dummy variables X_r used to discretize the radiation force, the position p and the velocity v of the device.

This model shows that wave elevation affects the device dynamics through (3), hence accurate knowledge of the wavefield is necessary whenever the dynamic behavior of the WEC device needs to be computed.

III. ENSEMBLE OCEAN WAVE FORECASTING

Ensemble Kalman Filtering is a powerful data assimilation scheme which has received growing appreciation in the weather forecasting community over the years, since the seminal paper by Evensen [5]. The extension to ocean wave forecasting is rather straightforward. A specified number of ensemble members N_{KF} is initially generated by randomly sampling a sea spectrum assumed to approximately represent the actual sea state. Then, a mathematical model of the wave process is employed to advance each member independently over time. Whenever new measurements of the wavefield becomes available, first and second order statistics are calculated from the ensemble set to perform the Kalman Filter assimilation step. Afterward, the updated members are again propagated in time until new measurements become available.

In the present work, the dynamic model adhibited to the time propagation of the actual and ensemble wavefields has been derived from linear wave theory. Under the assumption of inviscid flow, finite-depth water, linear wave interaction, and constant atmospheric pressure at the interface between air and water, wave dynamics is completely described by the following pair of equations

$$\begin{cases}
\frac{\partial \eta}{\partial t} = -\mathcal{L}\left[\Phi\right] \\
\frac{\partial \Phi}{\partial t} = -g \eta
\end{cases}$$
(7)

where $\eta(x,\,y,\,t)$, is the the wave elevation and $\Phi(x,\,y,\,t)$ is the surface scalar flow potential at the horizontal spatial coordinates x and y over time t. The operator $\mathcal{L}\left[\Phi\right]$ is defined as

$$\mathcal{L}\left[\Phi\right] = -\mathcal{F}^{-1}\left[k \, \tanh\left(k \, h\right) \mathcal{F}\left[\Phi\right]\right] \tag{8}$$

in which $\mathcal{F}[\cdot]$ denotes Fourier transform, k is the spatial wavenumber spanning Fourier domain, and h is the sea depth. In order to simplify the computation of the operator $\mathcal{L}[\cdot]$, a pseudospectral approach is adopted for the numerical implementation. This allows to leverage Fast Fourier Transform (FFT) routines resulting in increased computational speed. Introducing the state vector $x_{KF} = [\eta^T, \Phi^T]^T$ and denoting with \hat{x}_{KF} its Fourier transform, the system of equations in (7) can be expressed as

$$\dot{\hat{x}}_{KF}(t) = \begin{bmatrix} 0 & k \tanh(kh) \\ -g & 0 \end{bmatrix} \hat{x}_{KF}(t) \tag{9}$$

In this way, the propagation of the ensemble members can be carried out entirely in Fourier domain and transformation back to the physical space is needed only to perform the assimilation step.

In order to initialize the simulation of the actual sea state and the propagation of the ensemble members, the initial wave elevation $\eta_0(x,y)$ and flow potential $\Phi_0(x,y)$ need to be defined. In order to generate a wavefield which is representative of a realistic sea condition, we assume that the initial wavefield spectrum follows a JONSWAP distribution [6]. This semi-empirical model has been proved to provide a good approximation of the frequency spectrum of wind-generated waves in deep water. Following [7], the JONSWAP spectrum is defined as:

$$S(\omega) = 155 \frac{H_{1/3}^2}{T_p^4 \omega^5} e^{\frac{-944}{T_p^4 \omega^5}} \gamma^Y,$$
with $Y = e^{\frac{-(0.191 \omega T_p - 1)^2}{2 \sigma^2}},$
and $\sigma = \begin{cases} 0.07, & \omega \le 5.24/T_p \\ 0.09, & \omega > 5.24/T_p \end{cases}$ (10)

where $H_{1/3}$ is the significant wave height, T_p the dominant wave period, and γ the peak enhancement factor, which ranges from 1 for fully-developed sea states to 3.3 for developing sea state. The initial wavefield is then obtained by randomly selecting N_w harmonic components from the JONSWAP distribution in (10) and adding a uniformly random phase shifting to each component. The initial sea state $\eta_0(x,y)$ is then defined as

$$\eta_0(x, y) = \sum_{j=1}^{N_w} \sqrt{2S(\omega_j)\Delta\omega} \cos(k_j \cos \psi_0 x + k_j \sin \psi_0 y + \varepsilon_j)$$
(11)

where $\Delta\omega$ is the spectrum frequency resolution, ψ_0 accounts for the direction of the wave propagation, ε_j is a uniformly random phase shift ranging from 0 to 2π , and k_j is the wavenumber associated to each selected frequency component ω_j through the linear finite-depth wave dispersion relationship

$$\omega_j = \sqrt{gk_j \tanh(k_j h)} \tag{12}$$

The initial flow potential $\Phi_0(x, y)$ is then obtained through the solution of the linear wave propagation problem for the time series in (11):

$$\Phi_0(x, y) = \sum_{j=1}^{N_w} \frac{g}{\omega_j} \sqrt{2S(\omega_j)\Delta\omega} \sin(k_j \cos \psi_0 x + k_j \sin \psi_0 y + \varepsilon_j)$$
(13)

Likewise, the ensemble members are generated through Equations (11) and (13) by randomly sampling a perturbed version of the JONSWAP spectrum defined to generate the actual initial wavefield.

For the data assimilation step, measurements are supposed to be provided by a Doppler radar positioned at the device location. Such wave radar gives the radial component of the wavefield velocity $v_r(r,\,\theta\,,t)$, with respect to the radar local coordinates, at a specified sampling time. From the radar velocity, it is possible to directly calculate the surface potential within the radar range, through integration over the radial coordinate, i.e.

$$\Phi_m(r, \theta, t) = \int_0^r v_r(\rho, \theta, t) d\rho, \quad \text{for} \quad r \in [0, r_{\text{max}}]$$
(14)

in which $r_{\rm max}$ is the radar range. For simplicity, the center of the polar reference system is considered at the wave radar location. A linear interpolation is then performed in order to switch from the radar reference system to the Cartesian grid defined for the numerical simulation of the wave propagation equations. In order to represent the actual signal-to-noise ratio of a real wave radar measurements, which is known from theory to degrade with the fourth power of the distance from the center of the radar, a distance-dependent gaussian noise is introduced. Hence, the measurement noise covariance σ_R^2 is defined as:

$$\sigma_R^2(r) = \alpha + \beta \left(\frac{r}{r_{\text{max}}}\right)^4 \tag{15}$$

The data assimilation step is then performed using Kalman Filter update equations. Denoting with X_{KF} the matrix containing the ensemble set, the assimilation of radar measurements is performed at each sampling time, according to the following:

$$X_{KF}^{+} = X_{KF}^{-} + \frac{1}{N_{KF} - 1} V (CV)^{T}$$

$$\left[\frac{1}{N_{KF} - 1} (CV) (CV)^{T} + R \right]^{-1} (Y - CX_{KF}^{-})$$
(16)

where superscript — indicates the *prior* Ensemble Kalman estimation, while superscript + denotes the *posterior* Ensemble Kalman estimation, C is the measurement matrix relating radar measurements to the state-space vector x_{KF} , R the measurement noise covariance matrix defined according to (15), and Y is the matrix obtained after perturbing N_{KF} times the radar measurement vector with random noise consistent with the measurement noise statistics. Besides, we have

$$V = X_{KF}^{-} - E\left(X_{KF}^{-}\right) \tag{17}$$

where $E\left(X_{KF}^{-}\right)$ represents the first order statistics associated to the prior ensemble set.

Calculating the first order statistics of the ensemble set over the predefined control horizon, provides an estimate for the wave elevation at the device location $\bar{\eta}(t)$ in (3), to be leveraged in the MPC framework.

IV. MODEL PREDICTIVE CONTROL FOR OPTIMAL WEC POWER TAKE-OFF

Under the assumption of no losses in the power generation process, optimizing the WEC device average power take-off \bar{P}_a at a given instant t_0 over a defined control horizon T_h

can be achieved by determining the optimal control sequence u(t) maximizing the following cost function:

$$\bar{P}_a = -\frac{1}{T_h} \int_{t_0}^{t_0 + T_h} v(t) \, u(t) \, dt \tag{18}$$

where v is the device velocity. The minus sign is due to the convention of considering absorbed energy with a negative sign. After discretizing the integral in (18) and changing sign, the optimization problem now requires the minimization of

$$J = \frac{1}{N} \sum_{k=0}^{N-1} x_{k+1}^T S_v^T u_k \tag{19}$$

in which N is the number of time interval over the control horizon T_h , and S_v is a linear operator extracting the WEC velocity from the state-space vector. The control force and state vector, however, are not independent variables, and they are constrained by the dynamics equations of the WEC derived in (5), which in discrete time are defined as

$$x_{k+1} = A_d x_k + B_d u_k + B_d f_{ek}, \quad k = 0, ..., N-1$$
 (20)

with assigned initial condition $x_0 = \bar{x}_0$. In order to preserve mechanical and structural integrity, motion and machinery constraints are imposed, which limit the maximum actuation force and the WEC device velocity and vertical displacement for structural safety, i.e.

$$u_{\min} \le u_k \le u_{\max}, \quad k = 0, \dots, N - 1$$

 $p_{\min} \le S_p x_k \le p_{\max}, \quad k = 1, \dots, N$ (21)
 $v_{\min} \le S_v x_k \le v_{\max}, \quad k = 1, \dots, N$

where S_p is a linear operator extracting the WEC displacement from the state vector. The cost function in (19), together with the constraints in (20) and (21) represents a linear MPC problem in its standard formulation, as described in [8].

A more compact formulation can be obtained by defining the following vectors

$$\mathcal{X} = \begin{bmatrix} x_1^T, x_2^T, \dots, x_N^T \end{bmatrix}^T$$
$$\mathcal{U} = \begin{bmatrix} u_0^T, u_1^T, \dots, u_{N-1}^T \end{bmatrix}^T$$

In this way, the cost function can then be expressed as

$$J = \frac{1}{N} \mathcal{X}^T \mathcal{S}_v^T \mathcal{U} \tag{22}$$

The inequality constraints become

$$D_u \mathcal{U} \le d_u$$

$$D_x \mathcal{X} \le d_x$$
(23)

with

$$D_{u} = \begin{bmatrix} I \\ -I \end{bmatrix} \qquad d_{u} = \begin{bmatrix} u_{\text{max}} \\ -u_{\text{min}} \end{bmatrix}$$

$$D_{x} = \begin{bmatrix} \mathcal{S}_{p} \\ -\mathcal{S}_{p} \\ \mathcal{S}_{v} \\ -\mathcal{S}_{v} \end{bmatrix} \qquad d_{x} = \begin{bmatrix} p_{\text{max}} \\ -p_{\text{min}} \\ v_{\text{max}} \\ -v_{\text{min}} \end{bmatrix}$$

in which S_v and S_p are block-diagonal matrices having the velocity extraction matrix S_v and the position extraction

matrix S_p , respectively, on the main block-diagonal. By recursively applying the discrete-time dynamics equations in (20), it is possible to express \mathcal{X} as a function of the control vector \mathcal{U} , the excitation force vector \mathcal{F}_e , and the initial condition \bar{x}_0 , as done also in [3] and [9]:

$$\mathcal{X} = \mathcal{A}_d \, \bar{x}_0 + \mathcal{B}_d \, \mathcal{U} + \mathcal{B}_d \, \mathcal{F}_e \tag{24}$$

where

$$\mathcal{A}_{d} = \begin{bmatrix} A_{d} \\ A_{d}^{2} \\ \vdots \\ A_{d}^{N} \end{bmatrix} \quad \mathcal{B}_{d} = \begin{bmatrix} B_{d} & 0 & 0 & 0 \\ A_{d} B_{d} & B_{d} & 0 & 0 \\ \vdots & \vdots & \ddots & 0 \\ A_{d}^{N-1} B_{d} & A_{d}^{N-2} B_{d} & \cdots & B_{d} \end{bmatrix}$$

$$\mathcal{F}_{e} = \begin{bmatrix} f_{e0}^{T}, f_{e1}^{T}, \dots, f_{eN-1}^{T} \end{bmatrix}^{T}$$

Replacing relation (24) into (22) and (23) allows to rewrite the MPC problem as

$$\min_{\mathcal{U}} \quad \mathcal{U}^{T} \mathcal{B}_{d}^{T} \mathcal{S}_{v}^{T} \mathcal{U} + \left(\mathcal{S}_{v} \mathcal{A}_{d} \bar{x}_{0} + \mathcal{S}_{v} \mathcal{B}_{d} \mathcal{F}_{e}\right)^{T} \mathcal{U} \\
\left[\begin{matrix} D_{u} \\ D_{x} J_{u} \end{matrix} \right] \mathcal{U} \leq \left[\begin{matrix} d_{u} \\ d_{x} - D_{x} \mathcal{A}_{d} \bar{x}_{0} - D_{x} \mathcal{B}_{d} \mathcal{F}_{e} \end{matrix} \right]$$
(25)

Provided the Hessian of the cost function in (25) is positive definite, the maximization of power take-off requires the solution of a constrained convex optimization problem, for which well-consolidated routines, such as interior-point or active-set methods are available in literature (see [10] for an extensive review). As already observed in [3], positive definiteness of the Hessian is in general always guaranteed for the optimization of a point-absorber device, unless the time step chosen for the conversion of the continuous time model into discrete time turns out to be too large to represent the actual dynamic behavior of the WEC device.

At each timestep, an MPC problem like (25) needs to be solved, and the first value of the optimal solution vector \mathcal{U}^* is applied to the system. In this way, it is possible to achieve a real-time instantaneous optimization of the WEC device average power take-off. It has to be noticed, however, that, since the state vector x also contains the dummy variables used for the state space realization of the radiation force, the whole state is in general not available, and the initial condition \bar{x}_0 in the MPC optimization is not known and needs to be reconstructed through a state observer based on sensors placed on the device. Furthermore, as already mentioned in Section II, the excitation force vector \mathcal{F}_e is not available in real applications and needs to be estimated. The purpose of the Ensemble Kalman Filtering method derived in Section III is to provide an estimate $\hat{\mathcal{F}}_e$ over the MPC control horizon T_h .

V. RESULTS

We investigate the effect of ensemble wave forecasting on the MPC of the WEC device introduced in Section II for power take-off optimization. The structural parameters appearing in (6) have been defined as $m + m_{\infty} = 2 \cdot 10^6$, $r = 7 \cdot 10^4$, $k = 3 \cdot 10^6$, whereas radiation and excitation force impulse response functions $h_r(t)$ and $h_e(t)$ in (2)

and (3), respectively, have been derived using the boundary element code WAMIT [11]. For the simulation of the actual wavefield, a Cartesian domain of $4000\,m \times 4000\,m$ and a number of gridpoints equal to 256 in both directions is considered. The sea depth h is assumed constant and equal to $100\,m$.

For the propagation of the ensemble members a domain half of the size of the simulation domain is considered, while the spatial resolution is unchanged. For simplicity, the center of both domains have been placed at the device location. The overall simulation time is 200 s. An explicit fourthorder Runge-Kutta scheme has been implemented with a fixed timestep $\Delta t = 0.2 \, s$ for the time integration. The initial wavefield $\eta_0(x, y)$ in (11) has been obtained by randomly sampling the JONSWAP spectrum in (10) with $H_{1/3}$ = 2 m, $T_p = 8 s$, and $\gamma = 3.3$, while the initial ensemble members are obtained by sampling the same spectrum with a a randomly uniform perturbation of $\pm 20\%$ of the significant wave height $H_{1/3}$ and dominant period T_p . A number of ensemble members $N_{KF}=200$ has been employed. For the Doppler radar model, a range $r_{\text{max}} = 500 \, m$ is considered, with a radial and azimuthal resolution of 15 m and 2^o , respectively. The sampling time is 2s. For the measurement noise characterization in (15), we assume $\alpha = \beta = 10^{-2}$. In the MPC formulation, we impose actuator saturation at $u_{\rm max} = -u_{\rm min} = 10^7 \, N$, and motion constraints $p_{\rm max} =$ $-p_{\min} = 5 m$ and $v_{\max} = -v_{\min} = 5 m/s$. The control horizon T_h has been varied between one dominant wave period T_p and three times such period.

Results in Figure 2 show that EnKF provides overall good results with errors in the proximity of the device ranging from 5% of the actual wave elevation in case of pure estimation, up to 20% for forecasting at three times the dominant wave period. Interestingly, it is possible to observe the formation of a downstream wave of low-error estimation, due to the convection of the ensemble wavefield region of assimilation due to wave propagation.

The actual and estimated wave elevation at the device location $\bar{\eta}(t)$ and $\hat{\eta}(t)$ over the simulation time is shown in Figure 3. An average phase and amplitude error of nearly 2\% and 10%, respectively, has been observed. The average power take-off of the WEC device obtained over the simulation time leveraging MPC with full knowledge of the actual wavefield \bar{P}_a and with ensemble forecasting \hat{P}_a are shown in Figure 4 as a function of the control horizon T_h . Values have been normalized according to the asymptotic value of maximum power take-off, which has been calculated through the unconstrained infinite-time optimization of the continuous-time cost function in (18) in the linear optimal control setting. Results show that in case of full knowledge of the actual wavefield, a longer horizon always leads to better performance, eventually converging to the optimal control solution in the absence of active constraints. When the ensemble-based forecast is leveraged, a loss of 10% is observed for control optimization horizons T_h up to two dominant wave periods, and performance degrades to 16% for longer control optimization horizons, as the estimate

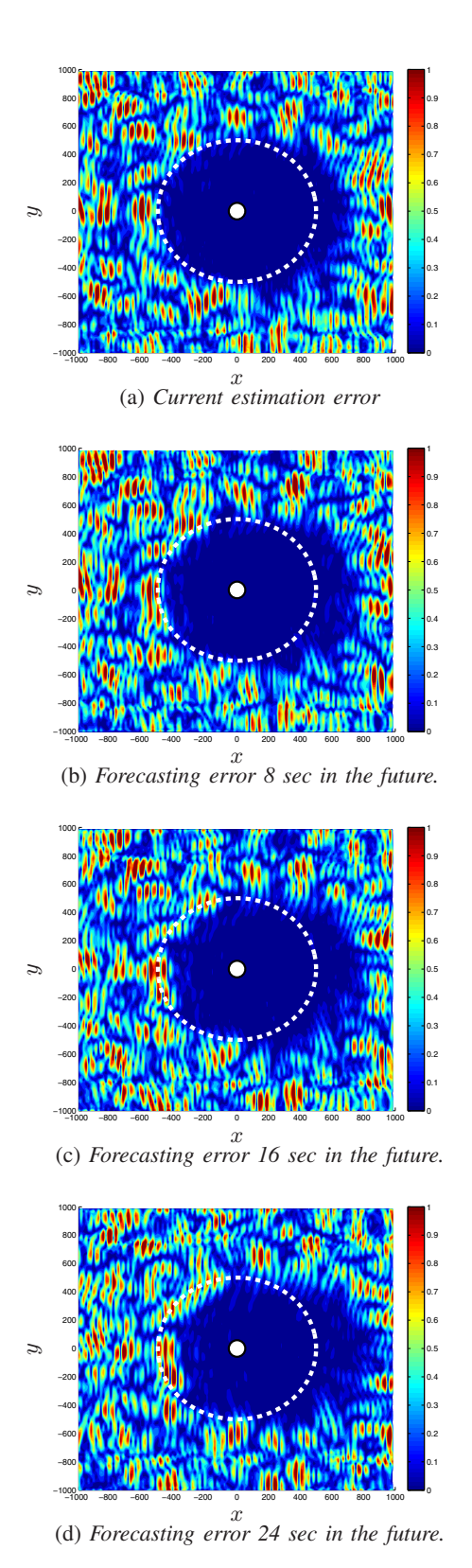


Fig. 2: Wave elevation prediction error (in meters) after $100\,s$ of simulation time at different forecast times. The white circle represents the WEC device, the white dashed line the radar range. Waves propagates from left to right, and the dominant wave period is $T_p=8~{\rm sec.}$

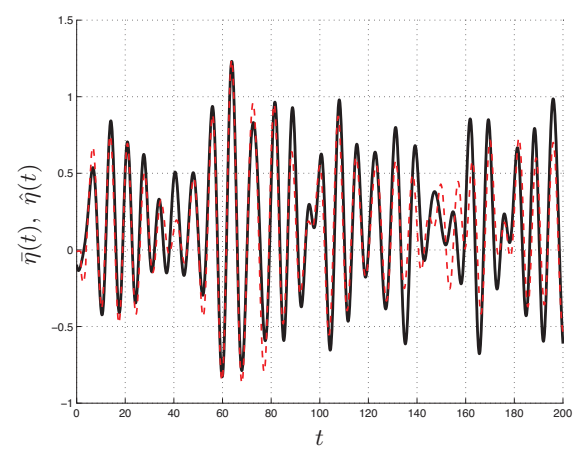


Fig. 3: Wave elevation at the device location: actual (solid black) and estimated (dashed red).

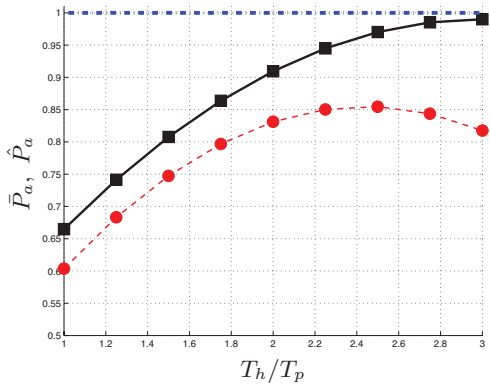


Fig. 4: Normalized WEC average power take-off: MPC with complete knowledge of the wavefield (solid black), and with ensemble forecasting (dashed red) with respect to the unconstrained infinite-time solution (dash-dotted blue).

of the wakefield further into the future is degraded. This is consistent to what found in [3]. A way to improve the performance of the coupled EnKF/MPC approach would be to increase the number of ensemble members N_{KF} , at the cost of increased computational time, or increase the radar range, or work with a wave measurement device with lower noise covariance, such as an array of measurement buoys placed upstream with respect to the WEC device.

VI. CONCLUSIONS

This paper represents one of the first attempts at developing a realistic MPC framework for the real-time optimization of the power take-off of a WEC device, through the implementation of an EnKF algorithm which assimilates data provided by a wave radar. Linear wave propagation theory is leveraged to forecast the wave elevation over the control optimization horizon, and an estimate of the excitation force is provided for the solution of the MPC problem. Results have shown that EnKF provides overall good results when applied to radar data assimilation for ocean wave prediction.

Simulations performed over a realistic sea state show that the power take-off obtained via MPC with exact knowledge of the actual excitation force approaches its maximum value when a control optimization horizon of at least three times the dominant wave period is considered, while when the EnKF estimation of such force is leveraged, a trade-off is present, since a longer control optimization horizon depends in a more sensitive fashion on the accuracy of the wavefield estimate.

The combined approach of ensemble wave forecasting and model predictive control of the WEC can easily be generalized to handle different scenarios. For example, the linear wave propagation model used here might prove inadequate at appropriately capturing the wave dynamics in certain settings, and a nonlinear wave interaction model or shallow water wave propagation model over an uneven bottom might be required. Different wave measurement devices can also be incorporated in the EnKF assimilation step, such as an array of wave measurement buoys surrounding the device. Moreover, the optimization of the power take-off of different WEC topologies allows an active control implementation to be handled in the linear MPC setting. In the case a linear approximation of the WEC device dynamics is insufficient, or in the presence of nonlinear constraints, the linear MPC formulation may be replaced by a more flexible nonlinear MPC approach. These extensions are currently underway, and will be reported in future publications.

ACKNOWLEDGEMENTS

We would like to thank Dr. Anantha Karthikeyan for providing the state-space model used for the simulations.

REFERENCES

- J. Falnes, Ocean waves and oscillating systems. Cambridge University Press, 2002.
- [2] J. Hals, J. Falnes, and T. Moan, "A comparison of selected strategies for adaptive control of wave energy converters," *Journal of Offshore Mechanics and Arctic Engineering*, vol. 133, no. 3, 2011.
- [3] —, "Constrained optimal control of a heaving buoy wave-energy converter," *Journal of Offshore Mechanics and Arctic Engineering*, vol. 133, no. 1, 2011.
- [4] Z. Yu and J. Falnes, "State-space modelling of a vertical cylinder in heave," *Applied Ocean Research*, vol. 17, no. 5, pp. 265–275, 1995.
- [5] G. Evensen, "The ensemble kalman filter: Theoretical formulation and practical implementation," *Ocean dynamics*, vol. 53, no. 4, pp. 343– 367, 2003.
- [6] K. Hasselmann, T. Barnett, E. Bouws, H. Carlson, D. Cartwright, K. Enke, J. Ewing, H. Gienapp, D. Hasselmann, P. Kruseman, et al., "Measurements of wind-wave growth and swell decay during the joint north sea wave project (jonswap)," 1973.
- [7] O. Faltinsen, Sea loads on ships and offshore structures. Cambridge university press, 1993, vol. 1.
- [8] J. M. Maciejowski, Predictive control with constraints. Pearson education, 2002.
- [9] M. Richter, "Different model predictive control approaches for controlling point absorber wave energy converters," *University Stuttgart*, Stuttgart, 2011.
- [10] S. Wright and J. Nocedal, *Numerical optimization*. Springer New York, 1999, vol. 2.
- [11] C.-H. Lee, WAMIT theory manual. Massachusetts Institute of Technology, Department of Ocean Engineering, 1995.